
MDS-ED: Multimodal Decision Support in the Emergency Department – a Benchmark Dataset for Diagnoses and Deterioration Prediction in Emergency Medicine

Juan Miguel Lopez Alcaraz

AI4Health Division

Carl von Ossietzky Universität Oldenburg

Oldenburg, Germany

juan.lopez.alcaraz@uol.de

Hjalmar Bouma

Department of Internal Medicine,
Department of Acute Care, and

Department of Clinical Pharmacy & Pharmacology

University Medical Center Groningen, University of Groningen

Groningen, Netherlands

h.r.bouma@umcg.nl

Nils Strothoff

AI4Health Division

Carl von Ossietzky Universität Oldenburg

Oldenburg, Germany

nils.strothoff@uol.de

Abstract

Background: Benchmarking medical decision support algorithms often struggles due to limited access to datasets, narrow prediction tasks, and restricted input modalities. These limitations affect their clinical relevance and performance in high-stakes areas like emergency care, complicating replication, validation, and improvement of benchmarks.

Methods: We introduce a dataset based on MIMIC-IV, benchmarking protocol, and initial results for evaluating multimodal decision support in the emergency department (ED). We use diverse data modalities from the first 1.5 hours of patient arrival, including demographics, biometrics, vital signs, lab values, and electrocardiogram waveforms. We analyze 1443 clinical labels across two contexts: predicting diagnoses with ICD-10 codes and forecasting patient deterioration.

Results: Our multimodal diagnostic model achieves an AUROC score over 0.8 in a statistically significant manner for 357 out of 1428 conditions, including cardiac issues like myocardial infarction and non-cardiac conditions such as renal disease and diabetes. The deterioration model scores above 0.8 in a statistically significant manner for 13 out of 15 targets, including critical events like cardiac arrest and mechanical ventilation, ICU admission as well as short- and long-term mortality. Incorporating raw waveform data significantly improves model performance, which represents one of the first robust demonstrations of this effect.

Conclusions: This study highlights the uniqueness of our dataset, which encompasses a wide range of clinical tasks and utilizes a comprehensive set of features collected early during the emergency after arriving at the ED. The strong performance, as evidenced by high AUROC scores across diagnostic and deterioration targets, underscores the potential of our approach to revolutionize decision-making in acute and emergency medicine.

1 Introduction

Artificial intelligence (AI) is an emerging field that has significantly enhanced healthcare and medicine [1] in areas such as precision medicine [2] and drug discovery [3]. The implementation of AI models is particularly relevant in acute and emergency medicine, where clinicians must address critical conditions within short time frames to make optimal clinical decisions. AI models can improve acute care by enabling early diagnosis [4], proposing tailored diagnostic workups [5], predicting admissions (including ward or intensive care unit (ICU)) [6], estimating survival rates [7], and providing faster and low-cost diagnoses [8]. There has been exponential growth in the number of scientific publications on new AI models. However, many of these studies have limitations, such as predicting only a limited set of specific conditions [9, 4], offering short time horizons for survival predictions, and requiring costly diagnostic tests [10].

Healthcare datasets are essential for advancing medical research and innovation. However, much of this valuable data remains undisclosed due to commercial interests and privacy concerns. Despite these hurdles, there has been a recent surge in publicly accessible datasets aimed at facilitating the development and validation of machine learning models to tackle complex healthcare challenges [11, 12, 13, 14, 15]. Nonetheless, these datasets still have limitations, including size constraints [12], lack of open-source availability [16, 17], and narrow scopes in terms of prediction tasks [12, 13, 17, 14, 16, 15]. Benchmarking is crucial for evaluating the performance and reliability of novel AI-models, ensuring their applicability and robustness in real-world clinical settings. In this study, we investigate multimodal decision support for emergency department (MDS-ED) using an open-source biomedical multimodal dataset which comprises various medical feature modalities, to predict a diverse and large range of clinical tasks beyond traditional predictive scenarios, such as cardiac and non-cardiac diagnoses, as well as patient deterioration such as mortalities, ICU admission, organ-specific failure, and mechanical ventilation to name a few.

2 Methods

2.1 Clinical workflow and dataset creation

Figure 1 presents a schematic illustration of the proposed MDS-ED pipeline which task focuses on a specific workflow with high clinical relevance, where for each ED visit, it encompasses a set of features collected from a window of 90 minutes from the patient’s arrival at the ED to predict patient discharge diagnoses and deterioration through the stay. MDS-ED was created by linking ECG waveforms from the MIMIC-IV-ECG [18] dataset to clinical features and outcomes as clinical ground truth from the MIMIC-IV and MIMIC-IV-ED dataset [19].

Prediction tasks and targets In this work, we broadly categorize all prediction tasks into two groups: patient discharge diagnoses and patient deterioration. For discharge diagnoses, we follow MIMIC-IV-ECG-ICD [11], which proposed a framework to predict discharge diagnoses based on a single electrocardiogram (ECG). To this end, we frame the task as a multilabel classification task in terms of ICD-10 CM codes. As in [11], we convert ICD-9 to ICD-10 CM codes where necessary, convert codes to 5 digits and propagate codes to parent codes up to the third digit. In this way, we obtain a total set of 1428 significantly populated ICD-10 CM codes covering a wide range of cardiac and non-cardiac conditions. For patient deterioration, we build on a consensus definition [20] and investigate 15 deterioration events in a multilabel setting after the patient arrived at different intervals and after the 1.5-hour feature collection window: Six subtasks cover clinical deterioration within 24 hours and cover severe hypoxemia, extracorporeal membrane oxygenation (ECMO), use of vasopressors, use of inotropes, mechanical ventilation, and in-hospital cardiac arrest (IHCA). Two subtasks cover ICU admission within 24 hours and or within the entire stay, and finally, 7 subtasks

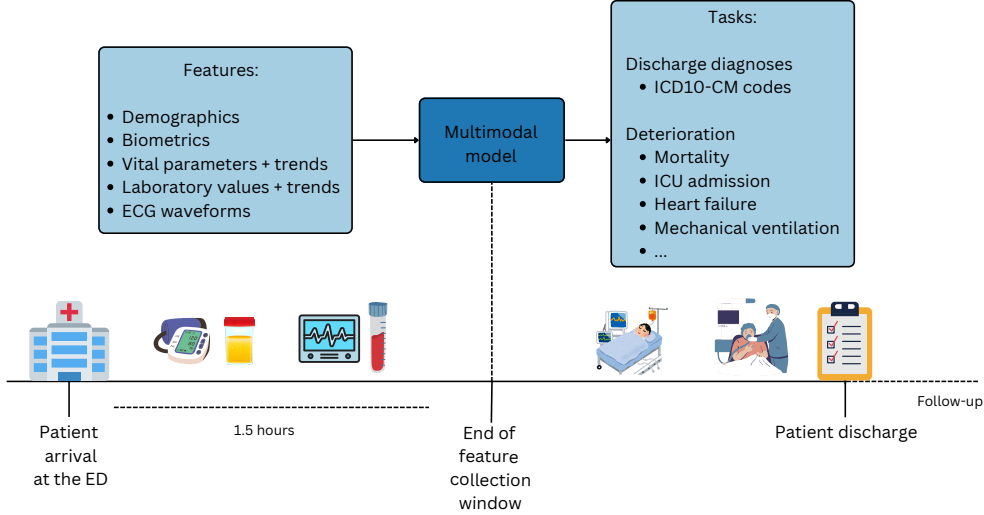


Figure 1: Pipeline outlines the MDS-ED workflow, which involves feature collection encompassing patient demographics, biometrics (such as height, weight, and BMI), vital parameters and trends, laboratory values and trends, and ECG waveform data to address two clinically relevant prediction scenarios: predicting patient discharge diagnoses out of 1428 cardiac and non-cardiac ICD10-CM codes and predicting patient deterioration according to 15 clinical deterioration measures.

cover mortality prediction at different horizons ranging from inpatient mortality, 24 hours, 7 days, 28 days, 90 days, 180 days, to 365 days. With these two main groups, we aim to cover a wide range spectrum of patient monitoring in the ED as well as long-term mortality across 1,443 unique target labels, see Table 5 in the supplementary material for a detailed target definition discussion.

Features While aiming to include mainly data at triage, we also include irregularly sampled vital parameters and lab values captured during the 1.5h data collection window. To capture trends, we compute simple sample-wise statistical aggregation functions per vital parameter and laboratory values, namely mean, median, minimum, maximum, standard deviation, first and last values, rate of change of them between first and last value, as well as the slope of a linear model fitted on the minutes difference between value collection and arrival as independent variable and the actual values as dependent variables. We follow [21] to select an appropriate set of laboratory values that avoids a bias towards particular prediction targets. We obtain a total of 470 features across all feature modalities in a tabular format plus a 12-lead 10-second ECG waveform per sample.

MDS-ED consists of data from 71,098 patients, encompassing 121,195 unique visits, and a total of 129,095 samples. We leverage the stratified splits provided along with the dataset accompanying [11], which includes stratification based on gender, age bins, and discharge diagnoses. We distribute the total number of 20 stratified folds into train, validation, and test following ratios of 18:1:1, see Appendix A in the supplementary material for further preprocessing and definitions details as well as descriptive statistics on demographics, biometrics, vital parameters and laboratory values in Tables 6-8.

2.2 Related work

Table 1 contains a direct comparison with related works in terms of population, dataset size, features, availability, and number of target labels. [12] proposed the MIMIC-ED-Assist benchmark to reduce ED length of stay by flagging high-risk patients using triage features. [13] proposed VitalML to predict deterioration in the next 90 minutes from the first 15 minutes of monitoring. [17] proposed a multiple embedding model for EHR (MEME) to generate pseudo-notes from tabular data and predict ED disposition, discharge location, ICU admission, and inpatient mortality utilizing a natural language processing approach. [14] proposed a few shot foundational model EHRSHOT approach

Group	Detail	MIMIC-ED-Assist	VitalML	MEME	EHRSHOT	MC-BEC	MDS-ED
Source		[12]	[13]	[17]	[14]	[16]	This work
Population		ED	ED	Longitudinal	Longitudinal	ED	ED
Size	Patients Visits	25714 32356	N/A 19847	947028 N/A	6739 921499	63389 102731	71098 121195
Features	Demographics	✓	✓	✓	✓	✓	✓
	Biometrics	✗	✗	✗	✗	✗	✓
	Vital parameters	✓	✓(T)	✓(T)	✗	✓(T)	✓(T)
	Lab. values	✓	✗	✗	✓	✓(T)	✓(T)
	Waveforms	✗	✓(E)	✗	✗	✓	✓
	Chief complaint	✓	✗	✓	✗	✓	✗
	Medications	✗	✗	✓	✓	✓	✗
Tasks	Labels	3	3	4	15	7	1443
Availability	Open source	✓	✓	✗	✓	✗	✓

Table 1: Direct comparison with related works in terms of dataset size, features, availability, and number of target labels. We use diverse symbology to express the contribution where ✓ = available, ✗ = unavailable, E = available in the form of embeddings, and T = available in the form of trends or at least two sampled values.

to predict operational outcomes, developed diagnoses, as well as anticipate lab test results and image findings. [16] proposed MC-BEC to predict patient deterioration, disposition, and revisit from features collected including diagnoses from the first 15 minutes after the patient is assigned to a room.

Overall, our proposed MDS-ED main contributions in terms of the dataset are: **1) Comprehensive size:** MDS-ED is situated in the first position regarding a large number of patients and second in the number of visits in the open-source domain, despite restricting towards the investigated setting of the first 1.5 hours of ED arrival. **2) Diverse input features:** MDS-ED is situated in the first position in terms of feature modalities in the open-source domain as it incorporates a comprehensive set of features, including demographics, biometrics, vital parameter trends, laboratory values trends, and ECG waveforms. This is more extensive than most compared datasets. Intentionally, we decided to exclude chief complaints as their unstructured nature presents a more challenging step towards external validation with the addition of more variance, see [17]. Similarly, we exclude previous patient medications as they involve irregularities in administration times, and dosages, as well as potential bias towards task prediction, e.g., certain medications are given for specific gravity and stages of diagnoses. **3) Comprehensive prediction targets:** MDS-ED proposes 1,443 target labels, significantly more than other datasets, which typically cover fewer and too narrow in scope tasks. **4) Accessibility:** Similar to [12, 13, 14], MDS-ED is open source, encouraging further research and collaboration.

2.3 Model architectures

To propose an initial benchmark, we experiment with diverse settings based on data modalities input such as (1) tabular only, (2) ECG waveforms only, (3) ECG features + tabular, and (4) ECG waveforms + tabular. For waveforms (2) and (4), inspired by recent successful applications in the field of physiological time series [11, 22, 23] we employed an S4 classifier based on structured state space models with four layers [24], specifically, for the multimodal approach in (4) we extended the S4 classifier by fusing it with the tabular features using a tensor fusion approach based on a differentiable outer product proposed in the context of multimodal sentiment analysis [25]. For (1) and (3) we fit gradient-boosting decision trees (XGBoost). Additional details on model architectures and model hyperparameters can be found in Appendix B Table 9.

2.4 Training and evaluation

For the S4 models, we used AdamW as optimizer, with both learning rate and weight decay set to 0.001, and maintained a constant learning rate schedule. The training was conducted with a batch size of 64 samples over 20 epochs which usually converged earlier and model selection on the validation set. The training objective was to minimize binary cross-entropy loss. For all the models, we evaluate performances on the macro average across all areas under the respective receiver operating curves

(AUROC) (macro AUROC). To assess statistical uncertainty resulting from the finite size and specific composition of the test set, we employ empirical bootstrap on the test set with $n = 1000$ iterations. We report 95% confidence intervals for both macro AUROC and individual label AUROCs. Given [11] evaluation protocol, we use only the first record per visit per patient to avoid bias. Additional details of training and evaluation procedures can be found in Appendix B.

3 Results

3.1 Benchmarking predictive performance

	Diagnoses	Deterioration
Tabular only	0.7574 (0.7561, 0.7610)	0.8519 (0.8502, 0.8535)
ECG waveforms only	0.7631 (0.7590, 0.7673)	0.8279 (0.8047, 0.8511)
ECG features + Tabular	0.7684 (0.7673, 0.7721)	0.8693 (0.8688, 0.8715)
ECG waveforms + Tabular	0.7873 (0.7832, 0.7913)	0.8815 (0.8625, 0.8977)

Table 2: Predictive performance (macro AUROC with 95% bootstrap confidence intervals) across all tasks for unimodal models as well as multimodal prediction models.

Table 2 presents the predictive performance of both unimodal and multimodal models across the diagnoses and deterioration settings. For diagnosis prediction, the multimodal model that integrates ECG waveforms and tabular data achieved an AUROC of 0.7873 (0.7832, 0.7913), which significantly outperformed the unimodal models as well as the ECG features and tabular. Interestingly, the unimodal ECG waveforms model outperformed the unimodal tabular model with 0.7631 (0.7590, 0.7673) against 0.7574 (0.7561, 0.7610). In the deterioration prediction task, the multimodal model achieved an AUROC of 0.8815 (0.8625, 0.8977), which is notably higher than the unimodal models as well as the ECG features and tabular. Interestingly, contrary to the diagnoses setting, the tabular-only model outperformed the ECG waveform-only model with 0.8519 (0.8502, 0.8535) against 0.8279 (0.8047, 0.8511). In the following discussion, we restrict ourselves to the discussion of the most comprehensive multimodal model based on tabular features and ECG waveforms.

3.2 Task-dependent predictive performance

Table 3 demonstrates the diagnoses that can be predicted most accurately by the model, which we organized based on ICD chapters. The algorithm’s predictive performance ranges from an AUROC of 0.7282 for the Musculoskeletal System (XIII) chapter to 0.8467 for the Circulatory System (IX) chapter. In total, the model predicted 325 out of 1,242 individual ICD diagnoses with high accuracy, which we define in this work as conditions where the lower bound of the 95% bootstrap confidence interval for AUROC exceeding 0.80.

Table 4 showcases the deterioration model’s predictive performance across clinical deterioration, ICU admission, as well as both short and long-term mortality with many AUROC scores significantly exceeding the 0.80 threshold. Overall, for clinical deterioration, the model achieves an AUROC of 0.8692, whereas for ICU admissions, the model reports an overall AUROC of 0.8842, and for mortality predictions also exhibits high performance, with an overall AUROC of 0.9030.

4 Discussion

4.1 Impact of data modalities

From Section 3.1 we can draw several conclusions: Firstly, the results demonstrate that multimodal models, which integrate diverse data types, offer superior performance in both diagnostic and deterioration tasks (row 1/2 vs. row 3/4). Secondly, in the diagnoses task, the use of ECG raw waveforms instead of ECG features improves the performance in a statistically significant manner (row 3 vs. row 4), whereas for the deterioration task, we performed a direct comparison via bootstrapping the score difference for statistical significance, and we did not find a statistically

Code: AUROC [instances]. Description	Code: AUROC [instances]. Description
IX: Circulatory System. 0.8467 (93/181 >0.80 lower bound AUROC)	
I2119: 0.9975 [395] ST elevation (STEMI) myocardial infarction involving other coronary artery of inferior wall	I132: 0.9803 [871] Hypertensive heart and chronic kidney disease with heart failure and with stage 5 chronic kidney disease, or end stage renal disease
I081: 0.9793 [397] Rheumatic disorders of both mitral and tricuspid valves	I447: 0.9691 [1088] Left bundle-branch block, unspecified
I255: 0.9658 [946] Ischemic cardiomyopathy	I420: 0.9616 [315] Dilated cardiomyopathy
I481: 0.9549 [265] Persistent atrial fibrillation	I120: 0.9525 [3350] Hypertensive chronic kidney disease with stage 5 chronic kidney disease or end-stage renal disease
I30: 0.9514 [316] Acute pericarditis	I5023: 0.9494 [3216] Acute on chronic systolic (congestive) heart failure
III: Blood and immune mechanism: 0.8011 (14/45 >0.80 lower bound AUROC)	
D6181: 0.9333 [1503] Pancytopenia	D631: 0.9268 [2960] Anemia in chronic kidney disease
D6832: 0.9194 [271] Hemorrhagic disorder due to extrinsic circulating anticoagulants	D69: 0.8712 [5599] Purpura and other hemorrhagic conditions
IV: Endocrine, nutritional and metabolic. 0.801 (38/107 >0.80 lower bound AUROC)	
E1143: 0.9529 [249] Type 2 diabetes mellitus with diabetic autonomic polyneuropathy	E1022: 0.9393 [309] Type 1 diabetes mellitus with diabetic chronic kidney disease
E43: 0.9216 [1417] Unspecified severe protein-calorie malnutrition	E874: 0.9187 [632] Mixed disorder of acid-base balance
XIV: Genitourinary system 0.7978 (12/39 >0.80 lower bound AUROC)	
N186: 0.9594 [4362] End stage renal disease	N08: 0.9334 [798] Glomerular disorders in diseases classified elsewhere
N170: 0.906 [1773] Acute kidney failure with tubular necrosis	N2581: 0.8816 [472] Secondary hyperparathyroidism of renal origin
XIX: Injury, poisoning: 0.797 (20/84 >0.80 lower bound AUROC)	
S0180: 0.9143 [261] Unspecified open wound of other part of head	S063: 0.9125 [249] Focal traumatic brain injury
T8612: 0.9075 [559] Kidney transplant failure	T4551: 0.9021 [572] Poisoning by, adverse effect of and underdosing of anticoagulants
II: Neoplasms. 0.792 (6/53 >0.80 lower bound AUROC)	
C228: 0.9326 [236] Malignant neoplasm of liver, primary, unspecified as to type	C786: 0.9198 [490] Secondary malignant neoplasm of retroperitoneum and peritoneum
C83: 0.8825 [370] Non-follicular lymphoma	C7952: 0.8794 [629] Secondary malignant neoplasm of bone marrow
I: Infectious and parasitic diseases 0.7908 (7/51 >0.80 lower bound AUROC)	
A4189 0.9688 [267] Other specified sepsis	B9681 0.8749 [245] Helicobacter pylori [H. pylori] as the cause of diseases
X: Respiratory system. 0.7886 (23/71 >0.80 lower bound AUROC)	
J9691 0.9530 [572] Respiratory failure, unspecified with hypoxia	J152 0.9438 [289] Pneumonia due to staphylococcus
I841 0.9136 [353] Other interstitial pulmonary diseases with fibrosis	I948 0.9048 [369] Other specified pleural conditions
XXI: Health status and services 0.7884 (40/163 >0.80 lower bound AUROC)	
Z992 0.9681 [3224] Dependence on renal dialysis	Z902 0.9633 [265] Acquired absence of lung [part of]
Z681 0.9535 [853] Body mass index (BMI) 19.9 or less, adult	Z4502 0.9533 [345] Encounter for adjustment and management of automatic implantable cardiac defibrillator
XI: Digestive system 0.7825 (29/119 >0.80 lower bound AUROC)	
K7031: 0.9817 [485] Alcoholic cirrhosis of liver with ascites	K7290: 0.9605 [548] Hepatic failure, unspecified without coma
K758: 0.9299 [457] Other specified inflammatory liver diseases	K762: 0.9272 [350] Central hemorrhagic necrosis of liver
XII: Skin and subcutaneous tissue 0.7804 (5/25 >0.80 lower bound AUROC)	
L9750: 0.9303 [297] Non-pressure chronic ulcer of foot	L409: 0.8694 [239] Psoriasis
V: Mental and behavioral disorders 0.7719 (11/71 >0.80 lower bound AUROC)	
F500: 0.9856 [262] Anorexia nervosa	F1012: 0.9243 [625] Alcohol abuse with intoxication
F4310: 0.9050 [748] Post-traumatic stress disorder, unspecified	F1210: 0.8753 [396] Cannabis abuse, uncomplicated
XVIII: Symptoms, signs, and abnormal findings 0.7477 (19/167 >0.80 lower bound AUROC)	
R6521: 0.9561 [2545] Severe sepsis with septic shock	R5081: 0.9532 [406] Fever presenting with conditions classified elsewhere
R570: 0.9507 [981] Cardiogenic shock	R297: 0.9273 [290] National Institutes of Health Stroke Scale (NIHSS) score
XIII: Musculoskeletal system 0.7282 (8/66 >0.80 lower bound AUROC)	
M6282: 0.9224 [598] Rhabdomyolysis	M7966: 0.8944 [231] Pain in lower leg
M8580: 0.8931 [540] Other specified disorders of bone density and structure	M86 0.8838 [489] Osteomyelitis

Table 3: Best-performing individual statements organized according to selected ICD chapters under-scoring the breadth of accurately predictable statements. The table shows the four best-performing individual statements per ICD chapter (10 for chapter IX (Circulatory system diseases), 4 for the rest), where we show only AUROC scores above 0.85 and where also the lower bound of the 95% bootstrap confidence interval exceeds 0.80. To showcase the breadth of reliably predictable statements, we list only the best-performing statement per 3-digit ICD code.

significant difference, which is in line with [13]. To the best of our knowledge, this is the first statistically robust demonstration of the added value of raw waveform input against features for clinically relevant prediction tasks such as diagnoses prediction. Thirdly, the model building on ECG waveforms as only input outperforms the tabular-only model in the diagnostic setting, but not in the deterioration setting (row 1 vs. row 2). We hypothesize that this is due to the inclusion of tabular trends over time which aligns with the task definition of deterioration. We believe that the inclusion of multiple raw ECGs over time instead of just a single snapshot would allow us to capture more meaningful deterioration trends also from raw waveform data.

Label: AUROC [instances]	Label: AUROC [instances]
Clinical deterioration. 0.8620 (4/6 >0.80 lower bound AUROC)	
Severe hypoxemia: 0.5839 [555]	ECMO: 0.8705 [166]
Vasopressors: 0.9132 [1172]	Inotropes: 0.9079 [376]
Mechanical ventilation: 0.9394 [4230]	IHCA: 0.9576 [623]
ICU admission. 0.885 (2/2 >0.80 lower bound AUROC)	
24-hours: 0.8923 [15688]	Overall: 0.8777 [18872]
Mortality. 0.8970 (7/7 >0.80 lower bound AUROC)	
In-hospital: 0.8954 [99]	24-hours: 0.9512 [817]
7-days: 0.9149 [2275]	28-days: 0.9009 [5153]
90-days: 0.8850 [9300]	180-days: 0.8692 [12844]
365-days: 0.8629 [17761]	

Table 4: Detailed breakdown of model performance in the deterioration category.

4.2 Clinical significance

From Section 3.2, we conclude that our diagnostic models exhibit high predictive capabilities for both acute and chronic conditions. Acute conditions like ST elevation myocardial infarction, acute pericarditis, persistent atrial fibrillation, and acute kidney failure require rapid diagnosis and immediate intervention to prevent severe outcomes. The model’s strong performance in identifying these conditions highlights its potential to significantly impact patient care through timely and accurate diagnosis. Conversely, chronic conditions such as hypertensive heart and chronic kidney disease, ischemic cardiomyopathy, dilated cardiomyopathy, and end-stage renal disease benefit from ongoing management and long-term treatment strategies. The model’s ability to effectively predict these chronic conditions underscores its utility in supporting sustained patient monitoring and management, ultimately improving patient outcomes through consistent and reliable diagnostic support. As demonstrated in [11], even the model based only on ECG waveforms can reliably predict cardiac but most notably non-cardiac conditions. This applies even more to the multimodal model that involves clinical features as well as ECG waveforms.

Our deterioration model has major clinical relevance by enhancing early recognition of patient deterioration and supporting physician decisions in the emergency department. Its high predictive performance across various scenarios effectively identifies patients at risk for severe complications, which is crucial in acute and emergency medicine. The model’s ability to reliably predict clinically relevant indicators, such as vasopressor use, inotrope use, mechanical ventilation, and in-hospital cardiac arrest, enables healthcare providers to anticipate these events and implement early, tailored interventions. Additionally, its robust performance in predicting ICU admissions allows for better resource allocation, ensuring that patients who need intensive care receive it promptly while preventing unnecessary admissions. The model accurately predicts 24-hour in-hospital mortality and has high accuracy in predicting 365-day mortality, supporting clinical decision-making in prioritizing high-risk patients and discussing prognosis with families. Long-term mortality predictions aid in advanced care planning, such as deciding against ICU admission for patients with a short expected lifespan after discharge, and inform post-discharge planning and follow-up care to prevent readmissions and improve long-term health outcomes.

4.3 Limitations

Despite the promising results, there are several limitations to consider. Firstly, the presented models rely on the specifics of Beth Israel Deaconess Medical Center in terms of patient demographics, available resources, process characteristics, and data collection practices. We carefully quantify the statistical uncertainties of our results and are convinced of the robustness of our results for this particular scenario within the limits of a retrospective evaluation. However, we cannot make any statements about the transferability of our findings to other hospitals or deployment scenarios as this would require an external validation dataset, see [26] for a recent perspective on the role of external validation for clinical decision support. Secondly, the reliance on data collected within the first 1.5 hours of the ED visits may limit the model’s applicability. We deliberately decided to focus on this setting to keep the dataset homogeneous. However, there is also a clear clinical case for a prediction model only incorporating information available during triage. A similar dataset to the one proposed

could be created, but this task is left for future research. Thirdly, while we focus on the construction of a benchmark dataset and provide the first results for it, we do not provide any insights into the trained models beyond a discussion of the model performance for specific conditions. This could be achieved for example through attribution methods proposed in the context of explainable AI, however, mostly in uni-modular settings [27], to verify that the models do not exploit spurious correlations to reach their strong performance. Again, a detailed investigation also of causal vs. associational attributions along the lines of [28] is beyond the scope of this submission. Finally, although the open-source dataset fosters innovation, the implementation of a large-scale single end-to-end model with a wide range of target variables such as the diagnoses case might result in challenges during deployment in resource-constrained hardware, see Appendix B in the supplementary material for a more extensive discussion.

4.4 Future research directions

The proposed dataset and benchmark protocol build on input parameters that are typically available in clinical workflows and address a set of comprehensive, clinically meaningful prediction tasks. We therefore envision it to represent a meaningful baseline to benchmark prediction algorithms in the field. An obvious extension would be to include free-text data along the lines of [15]. Going beyond MIMIC-IV, models developed on the proposed dataset could foreshadow the development of more comprehensive models on more specialized datasets such as [29], for example including molecular data as input and/or prediction targets, to address more fine-grained diagnostic or deterioration prediction targets.

4.5 Social impact

Clinically, these models enhance decision-making by providing timely and accurate predictions, reducing diagnostic errors, and improving patient care, especially in high-stakes emergency settings. The open-source nature of the curated dataset fosters collaboration and innovation from diverse research communities, allowing for the development of new models and tools that aim to improve benchmark scores and enable more direct comparisons across models. However, questions of algorithmic fairness remain to be investigated in detail in future work.

4.6 Authors contribution statement

JMLA and NS conceived and designed the project. JMLA conducted the full experimental analyses, with NS supervising them, and HB providing critical revision for clinical intellectual content. JMLA produced the first draft, NS and HB revised it. All authors critically revised the content and approved the final version for publication.

4.7 Code and data availability

Code for experiment reproducibility and dataset instructions in a dedicated code repository [30]. For easier usage, the dataset is currently prepared for submission as a Physionet dataset.

References

- [1] P. Rajpurkar, E. Chen, O. Banerjee, and E. J. Topol, “Ai in health and medicine,” *Nature Medicine*, vol. 28, no. 1, p. 31–38, Jan. 2022, doi: 10.1038/s41591-021-01614-0.
- [2] K. B. Johnson, W.-Q. Wei, D. Weeraratne, M. E. Frisse, K. Misulis, K. Rhee, J. Zhao, and J. L. Snowdon, “Precision medicine, ai, and the future of personalized health care,” *Clinical and translational science*, vol. 14, no. 1, pp. 86–93, 2021, doi: 10.1111/cts.12884.
- [3] S. Dara, S. Dhamercherla, S. S. Jadav, C. M. Babu, and M. J. Ahsan, “Machine learning in drug discovery: a review,” *Artificial Intelligence Review*, vol. 55, no. 3, pp. 1947–1999, 2022, doi: 10.1007/s10462-021-10058-4.
- [4] S. Hong, S. Lee, J. Lee, W. C. Cha, K. Kim *et al.*, “Prediction of cardiac arrest in the emergency department based on machine learning and sequential characteristics: model development and retrospective clinical validation study,” *JMIR medical informatics*, vol. 8, no. 8, p. e15932, 2020, doi: 10.2196/15932.
- [5] F. Harrou, A. Dairi, F. Kadri, and Y. Sun, “Forecasting emergency department overcrowding: A deep learning framework,” *Chaos, Solitons & Fractals*, vol. 139, p. 110247, 2020, doi: 10.1016/j.chaos.2020.110247.
- [6] M. Covino, C. Sandroni, M. Santoro, L. Sabia, B. Simeoni, M. G. Bocci, V. Ojetto, M. Candelli, M. Antonelli, A. Gasbarrini *et al.*, “Predicting intensive care unit admission and death for covid-19 patients in the emergency department using early warning scores,” *Resuscitation*, vol. 156, pp. 84–91, 2020, doi: 10.1016/j.resuscitation.2020.08.124.
- [7] P. Wang, Y. Li, and C. K. Reddy, “Machine learning for survival analysis: A survey,” *ACM Computing Surveys (CSUR)*, vol. 51, no. 6, pp. 1–36, 2019, doi: 10.1145/3214306.
- [8] S. Henna and J. M. L. Alcaraz, “From interpretable filters to predictions of convolutional neural networks with explainable artificial intelligence,” *arXiv preprint arXiv:2207.12958*, 2022.
- [9] R. A. Taylor, C. L. Moore, K.-H. Cheung, and C. Brandt, “Predicting urinary tract infections in the emergency department with machine learning,” *PloS one*, vol. 13, no. 3, p. e0194085, 2018, doi: 10.1371/journal.pone.0194085.
- [10] E. J. Hwang, J. G. Nam, W. H. Lim, S. J. Park, Y. S. Jeong, J. H. Kang, E. K. Hong, T. M. Kim, J. M. Goo, S. Park *et al.*, “Deep learning for chest radiograph diagnosis in the emergency department,” *Radiology*, vol. 293, no. 3, pp. 573–580, 2019, doi: 10.1148/radiol.2019191225.
- [11] N. Strodthoff, J. M. Lopez Alcaraz, and W. Haverkamp, “Prospects for artificial intelligence-enhanced electrocardiogram as a unified screening tool for cardiac and non-cardiac conditions: an explorative study in emergency care,” *European Heart Journal-Digital Health*, p. ztae039, 2024, doi: 10.1093/ehjdh/ztae039.
- [12] L. Sun, A. Agarwal, A. Kornblith, B. Yu, and C. Xiong, “Ed-copilot: Reduce emergency department wait time with language model diagnostic assistance,” *arXiv preprint arXiv:2402.13448*, 2024.
- [13] S. Sundrani, J. Chen, B. T. Jin, Z. S. H. Abad, P. Rajpurkar, and D. Kim, “Predicting patient decompensation from continuous physiologic monitoring in the emergency department,” *NPJ Digital Medicine*, vol. 6, no. 1, p. 60, 2023, doi: 10.1038/s41746-023-00803-0.
- [14] M. Wornow, R. Thapa, E. Steinberg, J. Fries, and N. Shah, “Ehrshot: An ehr benchmark for few-shot evaluation of foundation models,” *Advances in Neural Information Processing Systems*, vol. 36, 2024.
- [15] P. Hager, F. Jungmann, R. Holland, K. Bhagat, I. Hubrecht, M. Knauer, J. Vielhauer, M. Makowski, R. Braren, G. Kaassis *et al.*, “Evaluation and mitigation of the limitations of large language models in clinical decision-making,” *Nature medicine*, pp. 1–10, 2024, doi: 10.1038/s41591-024-03097-1.
- [16] E. Chen, A. Kansal, J. Chen, B. T. Jin, J. Reisler, D. E. Kim, and P. Rajpurkar, “Multimodal clinical benchmark for emergency care (mc-bec): A comprehensive benchmark for evaluating foundation models in emergency medicine,” in *Advances in Neural Information Processing Systems*, A. Oh, T. Naumann, A. Globerson, K. Saenko, M. Hardt, and S. Levine, Eds., vol. 36. Curran Associates, Inc., 2023, pp. 45 794–45 811.

- [17] S. A. Lee, S. Jain, A. Chen, A. Biswas, J. Fang, A. Rudas, and J. N. Chiang, “Multimodal clinical pseudo-notes for emergency department prediction tasks using multiple embedding model for ehr (meme),” *arXiv preprint arXiv:2402.00160*, 2024.
- [18] B. Gow, T. Pollard, L. A. Nathanson, A. Johnson, B. Moody, C. Fernandes, N. Greenbaum, J. W. Waks, P. Eslami, T. Carbonati, A. Chaudhari, E. Herbst, D. Moukheiber, S. Berkowitz, R. Mark, and S. Horng, “Mimic-iv-ecg: Diagnostic electrocardiogram matched subset,” 2023, doi: 10.13026/4nqg-sb35.
- [19] A. E. W. Johnson, L. Bulgarelli, L. Shen, A. Gayles, A. Shammout, S. Horng, T. J. Pollard, S. Hao, B. Moody, B. Gow, L. wei H. Lehman, L. A. Celi, and R. G. Mark, “MIMIC-IV, a freely accessible electronic health record dataset,” *Scientific Data*, vol. 10, no. 1, Jan. 2023, doi: 10.1038/s41597-022-01899-x.
- [20] O. J. L. Mitchell, M. Dewan, H. A. Wolfe, K. J. Roberts, S. Neefe, G. Lighthall, N. A. Sands, G. Weissman, J. Ginestra, M. G. S. Shashaty, W. D. Schweickert, and B. S. Abella, “Defining physiological decompensation: An expert consensus and retrospective outcome validation,” *Critical Care Explorations*, vol. 4, no. 4, p. e0677, Apr. 2022, doi: 10.1097/cce.0000000000000677.
- [21] M. Moor, N. Bennett, D. Plečko, M. Horn, B. Rieck, N. Meinshausen, P. Bühlmann, and K. Borgwardt, “Predicting sepsis using deep learning across international sites: a retrospective development and validation study,” *EClinicalMedicine*, vol. 62, 2023, doi: 10.1016/j.eclinm.2023.102124.
- [22] T. Wang and N. Strothoff, “S4sleep: Elucidating the design space of deep-learning-based sleep stage classification models,” *arXiv preprint arXiv:2310.06715*, 2023.
- [23] T. Mehari and N. Strothoff, “Towards quantitative precision for ecg analysis: Leveraging state space models, self-supervision and patient metadata,” *IEEE Journal of Biomedical and Health Informatics*, 2023, doi: 10.1109/JBHI.2023.3310989.
- [24] A. Gu, K. Goel, and C. Ré, “Efficiently modeling long sequences with structured state spaces,” in *International Conference on Learning Representations*, 2022.
- [25] A. Zadeh, M. Chen, S. Poria, E. Cambria, and L.-P. Morency, “Tensor fusion network for multimodal sentiment analysis,” *arXiv preprint arXiv:1707.07250*, 2017.
- [26] H. M. la Roi-Teeuw, F. S. van Royen, A. de Hond, A. Zahra, S. de Vries, R. Bartels, A. J. Carriero, S. van Doorn, Z. S. Dunias, I. Kant, T. Leeuwenberg, R. Peters, L. Veerhoek, M. van Smeden, and K. Luijken, “Don’t be misled: 3 misconceptions about external validation of clinical prediction models,” *Journal of Clinical Epidemiology*, vol. 172, p. 111387, Aug. 2024, doi: 10.1016/j.jclinepi.2024.111387.
- [27] G. Ott, Y. Schaubelt, J. M. Lopez Alcaraz, W. Haverkamp, and N. Strothoff, “Using explainable ai to investigate electrocardiogram changes during healthy aging—from expert features to raw signals,” *Plos one*, vol. 19, no. 4, p. e0302024, 2024, doi: 10.1371/journal.pone.0302024.
- [28] J. M. L. Alcaraz and N. Strothoff, “Causalconceptts: Causal attributions for time series classification using high fidelity diffusion models,” *arXiv preprint arXiv:2405.15871*, 2024.
- [29] E. Ter Avest, B. C. van Munster, R. J. van Wijk, S. Tent, S. Ter Horst, T. T. Hu, L. E. van Heijst, F. S. van der Veer, F. E. van Beuningen, J. C. Ter Maaten *et al.*, “Cohort profile of acutelines: A large data/biobank of acute and emergency medicine,” *BMJ open*, vol. 11, no. 7, p. e047349, 2021, doi: 10.1136/bmjopen-2020-047349.
- [30] J. M. L. Alcaraz and N. Strothoff, “AI4HealthUOL/MDS-ED,” <https://github.com/AI4HealthUOL/MDS-ED>, 2024, [Accessed 18-06-2024].

A Dataset details

Name	Labels	Details
Diagnoses model (1428 labels, based on [11])		
Diagnoses	1428	Discharge diagnoses ICD10-CM codes
Deterioration model (15 labels, based on [20])		
Mortalities	6	1, 7, 30, 90, 180, 365 days and in-stay
ICU Admission	2	24 hours and in-stay
Vasopressors	1	Within 24 hours: epinephrine, norepinephrine, vasopressin, dobutamine, dopamine, or phenylephrine
Inotropes	1	Within 24 hours: epinephrine, dobutamine, or dopamine
Mechanical Ventilation	1	Same day or next day ICD9/ICD10 codes: 9670, 9671, 9672, 5A1935Z, 5A1945Z, and 5A1955Z
In-Hospital Cardiac Arrest (IHCA)	1	Same day or next day ICD9/ICD10 codes: I469, 4275, I462, V1253, I468
Extracorporeal Membrane Oxygenation (ECMO)	1	Same day or next day ICD9/ICD10 codes: 3961, 3965, 3966, 5A1221Z, 5A1522G, 5A1522H, 5A15223, 5A1522F, 5A15A2F, 5A15A2G, and 5A15A2H
Severe Hypoxemia	1	Oxygen saturation \leq 85% within 24 hours

Table 5: Definitions of labels for the diagnoses and deterioration models, including 1428 discharge diagnoses based on ICD10-CM codes in the diagnoses model, and 15 labels covering clinical outcomes such as mortalities, ICU admission, vasopressors, inotropes, mechanical ventilation, in-hospital cardiac arrest (IHCA), extracorporeal membrane oxygenation (ECMO), and severe hypoxemia in the deterioration model.

Table 5 contains the considered tasks by description, number of labels, and additional details such as target criteria definition. Apart from diagnoses, we use the rest of the tasks defined as patient deterioration based on previous work from the literature that defines physiological deterioration [20]. Although we consider diverse scores such as SOFA significant, calculating these markers requires a more detailed definition of downstream task prediction, which goes beyond the scope of maintaining homogeneity across tasks in this study. The curation of the dataset starts from MIMIC-IV-ECG-ICD [11], from which we obtained the ICD10 diagnoses codes for the complete MIMIC-IV-ECG [18] dataset, therefore, based on ECG records with available ED stay_id, we select the ones that happened between the patient in time and the 1.5 hours window. Mortalities at finite horizons were computed based on the date of death from [18], and for the computation of mortality per stay we include discharge date times from the admissions table in [19] MIMIC-IV to account for final discharge, all of the mortalities dates were previously validated from the source with a follow-up up to 1 year after the patient’s last recorded discharge. ICU admission in 24 hours and per stay were computed based on the ICU stays table from [19]. Mechanical ventilation and ECMO were computed given the procedures table from MIMIC-IV-ED given the patient admission and procedure date. Cardiac arrest was computed from the diagnosis tables from MIMIC-IV-ED and MIMIC-IV, where we first validated if the patient was discharged with the diagnosis code within the ED or hospital otherwise. We clarify that although mechanical ventilation, ECMO, and cardiac arrest do not provide an exact time of events, we carefully approximate the times with dates given the same day or the day after. Vasopressors and inotropes were computed from the pyxis table from MIMIC-IV-ED given the exact time of the applied medication. Finally, severe hypoxemia was computed from the vital signs table from MIMIC-IV-ED. In the deterioration setting, to not discard samples where the events happened before the 1.5 hours for a single task, e.g. severe hypoxemia within 1.5 hours, we include a special token for the task in the label space which we mask during training and evaluation in order not to negatively affect training and evaluation for other labels due to exclusion of entire patients, see Appendix B for more details.

Name	Values
Gender (%)	
Female	68289 (52.9)
Male	60806 (47.1)
Age (%)	
Median years (SD)	64 (28)
Quantile 1: 18-49	32634 (25.27)
Quantile 2: 50-64	34376 (26.62)
Quantile 3: 65-77	31821 (24.64)
Quantile 4: 78-101	30264 (23.44)
Ethnicity (%)	
White	78310 (60.66)
Black	27680 (21.44)
Hispanic	9230 (7.14)
Asian	4700 (3.64)
Other	9175 (7.10)

Table 6: Summary demographic characteristics across samples including gender distribution, age distribution (median with standard deviation and quartiles), and ethnicity distribution in the study population, presented as percentages.

Table 6 provides detailed demographic information on the study population, including gender, age, and ethnicity. The gender distribution shows a slightly higher proportion of females (52.9%) compared to males (47.1%). The age distribution is divided into four quantiles, with a median age of 64 years and a standard deviation of 28 years. Regarding ethnicity, the majority of the population is White (60.66%), followed by Black (21.44%), Hispanic (7.14%), Asian (3.64%), and individuals of other ethnicities (7.10%). This diverse demographic distribution ensures a comprehensive evaluation of the model across various patient groups. These variables were extracted from the `ed_stays` table from MIMIC-IV-ED.

Name	Unit	Minimum	Maximum	Median	IQR	Records
Biometrics						
BMI	kg/m ²	0	99.2	27.7	8.70	70321
Weight	kg	20.41	367.99	77.11	27.56	73646
Height	cm	64.99	387.09	167.64	15.23	32573
Vital parameters						
temperature	°C	13.3	44.72	36.6	0.55	77179
heartrate	bpm	0.0	570.0	84.0	30.0	153249
resprate	bpm	0.0	169.0	18.0	4.0	150525
o2sat	%	0.0	100.0	99.0	3.0	146140
sbp	mmHg	0.0	274.0	130.0	35.0	151346
dbp	mmHg	0.0	486.0	73.0	23.0	151254
Triage						
Acuity	level	1	5	2	1	126071

Table 7: Summary of statistics across samples for biometric measurements, vital parameters, and triage acuity levels, including minimum, maximum, median, interquartile range (IQR), and number of records for each variable.

Table 7 provides details on the biometrics, vital parameters, and triage values considered in this work, including the name, unit, minimum value, maximum value, median value, and the number of records. Dataset preprocessing includes weight and height conversion from pounds and inches to kilograms and centimeters. During the data cleaning process, we removed outliers and introduced missing values at various thresholds to ensure model computational convergence. The specific thresholds for outliers were as follows: temperature below and above 50 and 150 Fahrenheit degrees respectively.

Heart rate above 700, respiration rate above 300, oxygen saturation below 0 and above 100, diastolic and systolic blood pressures above 500. BMI above 100, weight below 20 or above 400, and height below 60 and above 400. The temperature unit was converted from Fahrenheit to Celsius, whereas weight from pounds to kilograms, and height from inches to centimeters. Biometrics features were extracted from the online medical records table from MIMIC-IV from which we match the closest value of a patient stay within 30 days of admission, otherwise missing. Vital parameters and acuity were extracted from the vital signs and triage tables of MIMIC-IV-ED.

Name	Unit	Minimum	Maximum	Median	IQR	Fluid	Records
Abs. Basophil Count	K/uL	0.0	9.2	0.04	0.03	Blood	36837
Abs. Eosinophil Count	K/uL	0.0	15.33	0.09	0.15	Blood	36838
Abs. Lymphocyte Count	K/uL	0.0	88.08	1.47	1.12	Blood	36909
Alanine Aminotransf.	IU/L	1.0	1999.0	22.0	22.0	Blood	29999
Albumin	g/dL	1.0	6.7	4.0	0.79	Blood	28324
Alkaline Phosphatase	IU/L	5.0	1985.0	85.0	51.0	Blood	29923
Aspartate Aminotransf.	IU/L	1.0	1996.0	29.0	29.0	Blood	29995
Bands	%	0.0	61.0	0.0	3.0	Blood	6057
Base Excess	mEq/L	-413.0	29.0	0.0	6.0	Blood	8011
Basophils	%	0.0	35.0	0.4	0.39	Blood	79386
Bicarbonate	mEq/L	2.0	50.0	24.0	5.0	Blood	79771
Bilirubin, Direct	mg/dL	0.0	45.5	1.0	2.5	Blood	1174
Bilirubin, Total	mg/dL	0.0	55.8	0.5	0.5	Blood	30098
C-Reactive Protein	mg/L	0.1	299.3	17.95	75.14	Blood	1108
Calcium, Total	mg/dL	0.0	79.2	9.2	0.79	Blood	30262
Carboxyhemoglobin	%	0.0	18.0	2.0	2.0	Blood	1078
Chloride	mEq/L	58.0	140.0	102.0	6.0	Blood	79855
Creatine Kinase (CK)	IU/L	8.0	1998.0	115.0	158.0	Blood	9588
CK, MB Isoenzyme	ng/mL	1.0	497.0	3.0	4.0	Blood	9272
Creatinine	mg/dL	0.0	43.0	1.0	0.5	Blood	82850
Eosinophils	%	0.0	75.0	1.3	2.1	Blood	79387
Fibrinogen, Functional	mg/dL	35.0	1348.0	298.5	161.5	Blood	2280
Free Calcium	mmol/L	0.48	3.31	1.08	0.12	Blood	1472
Glucose	mg/dL	3.8	1684.0	113.0	50.0	Blood	85022
Hematocrit	%	6.9	66.1	38.3	7.89	Blood	82490
Hemoglobin	g/dL	0.0	21.8	12.6	3.0	Blood	84890
INR(PT)	nan	0.75	24.0	1.1	0.30	Blood	44656
Lactate	mmol/L	0.3	25.2	1.8	1.20	Blood	32666
Lymphocytes	%	0.0	100.0	19.7	17.1	Blood	79387
Magnesium	mg/dL	0.2	45.0	2.0	0.40	Blood	30472
Neutrophils	%	0.0	99.0	69.9	19.59	Blood	79387
Oxygen Saturation	%	0.2	901.0	80.0	32.0	Blood	4838
PT	sec	8.2	150.0	12.0	3.5	Blood	44656
PTT	sec	16.6	150.0	30.6	6.99	Blood	44497
Phosphate	mg/dL	0.2	23.8	3.4	1.1	Blood	29888
Platelet Count	K/uL	5.0	1898.0	227.0	105.0	Blood	82260
Potassium	mEq/L	1.3	10.7	4.2	0.80	Blood	79857
RDW	%	10.6	33.8	13.8	2.19	Blood	82266
Red Blood Cells	m/uL	0.65	8.06	4.25	0.96	Blood	82266
Sodium	mEq/L	88.0	179.0	139.0	5.0	Blood	79865
Troponin T	ng/mL	0.0	17.36	0.06	0.13	Blood	41806
Urea Nitrogen	mg/dL	1.0	263.0	18.0	13.0	Blood	82522
White Blood Cells	K/uL	0.0	632.1	8.1	4.60	Blood	82367
pCO2	mm Hg	8.0	189.0	44.0	17.0	Blood	8008
pH	units	5.0	9.0	6.0	1.0	Urine	20968

Table 8: Summary of laboratory values across samples considered in this study, including the name, unit, minimum value, maximum value, median value, fluid type, and the number of records for each parameter.

Table 8 provides details on the laboratory values considered in this work, including the name, unit, minimum value, maximum value, median value, fluid type, and the number of records. During the data cleaning process, we removed outliers and introduced missing values at various thresholds to ensure

model computational convergence. The specific thresholds for outliers were as follows: absolute basophil count above 20, absolute eosinophil count above 20, absolute lymphocyte count above 100, alanine aminotransferase above 2000, alkaline phosphatase above 2000, aspartate aminotransferase above 2000, creatine kinase above 2000, glucose above 2000, lactate above 2000, and platelet count above 2000. Laboratory values were extracted from the laboratory events table from MIMIC-IV, where for each record we matched all the patient records of the desired tests available between patient record in-time and the 1.5 hours window.

B Models

Hyperparameter	Value
Block of layers	4
S4 model copies	512
S4 state size	8
Optimizer	Adam
Learning rate	0.001
Weight decay	0.001
learning rate schedule	constant
Batch size	64
Epochs	20

Table 9: S4 model hyperparameters

Table 9 outlines the hyperparameters employed in the S4 model. The architecture consists of four blocks of layers, with each block containing 512 copies of the S4 model. The state size within the S4 model is set to 8. For optimization, the AdamW optimizer is utilized with a learning rate and weight decay both set to 0.001. The learning rate schedule is maintained constant throughout training. A batch size of 64 samples is used for each training iteration, spanning a total of 20 epochs. The training objective is to minimize the binary cross-entropy loss. During training, we apply a model selection strategy on the best performance (AUROC) on the validation set which usually converges earlier than the final number of epochs. As previously described in Appendix A, with the goal of not discarding samples whose any of the deterioration targets happens before the 1.5-hour window or the target event cannot be clearly defined, we introduce a special token in the label space (-999) for which we account during training and evaluation to be discarded. As of XGboost models, we fit these models with the default hyperparameter values in a binary setting for the later AUROC aggregation across settings, models which in principle do not intrinsically allow the inclusion of samples during training with the special token to be discarded.